Electromagnetic scattering from layered strip geometries: the method of moments study with the sinc basis

Taner OĞUZER[1,*], **Fadıl KUYUCUOĞLU**[2], **İbrahim AVGIN**[2]
[1]*Department of Electrical and Electronics Engineering, Faculty of Engineering,*
Dokuz Eylül University, Buca, 35160 İzmir-TURKEY
e-mail: taner.oguzer@deu.edu.tr
[2]*Department of Electrical and Electronics Engineering, Faculty of Engineering,*
Ege University, Bornova, 35100 İzmir-TURKEY

Abstract

Electromagnetic scattering from strips of layers is analyzed using the method of moments (MoM) for both polarizations in spatial domain with the sinc-type orthogonal sets as basis and testing functions. We exploited the sinc function's properties of exponential convergence, the orthogonality, easy convolution and better handling of singular kernels in MoM procedure resulting in fast performance and reasonable accuracy even in ordinary MoM treatment. We transferred the integral of the Hankel function multiplied by sinc functions to Hankel function introducing a slight error with large band width. We proved that this relative error during the generation of the main matrix elements is smaller than that of the free space error, i.e., 1%–0.5% for considerably large matrix sizes. Our approach is readily applicable to a singular kernel problem due to properties of the sinc functions in particular 2D geometry. The procedure undertaken here is proven to be very efficient as regard to similar treatments in the literature developed mainly for regular kernels. Various numerical results are calculated such as the surface induced current and normalized far field radiation pattern. We compared them with the results available in the literature.

Key Words: *Electromagnetic scattering, layered media, computational electromagnetics*

1. Introduction

Electromagnetic modeling of various complexities require advanced numerical techniques such as the method of moments (MoM) [1], the finite element method (FEM) [2] and the finite difference time domain method (FDTD) [3]. Some efforts have gone to improve the classical problems, such as in [4], but requires tremendous computational capacity. The MoM reduces the original operator (i.e. differential or integral) to an algebraic

---

*Corresponding author: Department of Electrical and Electronics Engineering, Faculty of Engineering, Dokuz Eylül University, Buca, 35160 İzmir-TURKEY

linear equation. The MoM can be employed 3D and 2D geometries to the scattering and propagation of the printed strip and the slotted structures in layered media. Particularly even in 2D geometries the MoM method can be approximated by generalized pencil of functions (GPOF) [5] which enable us a closed form Greens functions in spatial domain for planar layered medium so that we save computational time. However both the spectral and spatial domain Green's functions have to be used in the MoM treatment [5].

The usual MoM formulation involves an integral equation (IE) which can be written for an electromagnetic problem either the mixed potential integral equation (MPIE) or the electric-field integral equation (EFIE) for open geometries. These equations contain the auxiliary vector and scalar potentials obtained through the appropriate Green's functions. The Green's functions in the spectral domain can be computed easily, whereas the Green's function in the spatial domain requires an efficient inverse Fourier transform algorithm. We also have to discretize the unknown current function by the known basis functions out of various configurations, i.e. pulse or triangle. The IE is discretized and then reduced by an error reduction technique (i.e., an inner product testing) to a system of an algebraic matrix equation. In 2D, the matrix elements can be computed either by double integrals in the spatial domain or single infinite integral in the spectral domain.

In the electromagnetic scattering problems the various techniques were applied to the strip scattering geometries as given in the [12, 13–14]. Also in [15] a different approach is presented as an effective one. Similarly 3D problems were studied as given in [16, 17]. In [18], the linear thin wire antennas are solved by radiation and scattering problems. In this study a wavelet based solution technique is used. On the other hand a regularized type solution is used in [19] for the strip scattering problem but it needs some complicated mathematical tasks. In all these studies, problems are solved for free space case and for layered geometries by using the effective computation of the Green's function as described below.

The closed form spatial domain Green's function in 3D for micro-strip structures are obtained in [6] and [7] by using an efficient tool, the GPOF in the usual MoM. A similar approach can be taken in 2D problems by expressing the Green's functions as a finite sum of Hankel functions [5].

We choose here the sinc type basis and testing functions as in [20–22, 24] when formulating the method of moments. The sinc functions consist of an orthogonal set with desirable properties: well suited numerically handling singularities and an exponential convergence with system size. A finite difference approach is taken when handling the derivatives in the problem since sinc method has a capacity making bunch up more points then the other methods.

The expansion of the unknown current density function in coefficients of the sinc function involves sampling it at the peak positions on the scatterer's surface. In the usual MoM with the Galerkin procedure, the sinc function integrals yield easy computation, for instance, the convolution of two sinc functions under integral produce a single sinc function. The use of the sinc collocation in the electromagnetic theory is a new approach. Lately it has been applied to Hallen's integral equation in [8] and to various boundary value problems, such as in [9, 10]. In [11], the surface scattering problem is also solved by the MoM using the sinc type basis as a sampling approach.

Here we used the sinc based MoM in the spatial domain and requires just one small term summation of the GPOF contrary to one integral and summation in the usual procedure [5]. We can calculate thus the main matrix elements as the sampled spatial domain Green's function values. Closed form Green's functions in spatial domain using the GPOF are given in the literature [5]. Therefore no integration is necessary except for some singular points of the Green's function. This allows one to compute the problem faster and with performance compared to that of the usual MoM. This is our main contribution to the problem studied here since the demand

from any technique is faster computation with reduced relative error in the main matrix calculations.

With sinc type functions, we have here considerable improvement in the CPU time and reasonably reduced error. In all these studies, the e^{jwt} convention is suppressed.

2. The closed-form Green's function for 2D layered media

Consider a planar multilayer as in Figure 1, where the transverse direction extends to infinity and a line source infinite in the y-direction that is buried in layer i. Any layer may be selected for the observation point. Each layer has its own relative electric and magnetic (ε_{ri}, μ_{ri}) constants and the layer thickness is d_i. Also, z and z' are the observation position and source points, respectively.
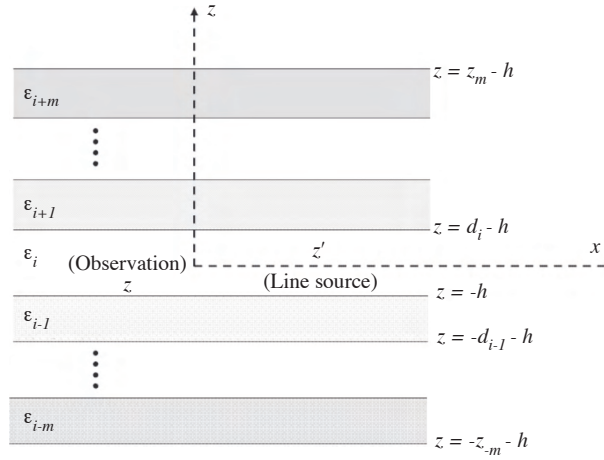

Figure 1. Layered geometry of the studied problem.

The spatial domain Green's function in 2D are discussed in [5] involving a line source $\vec{J} = \hat{y}\delta(\rho)$ for the E-polarization case and $\vec{J} = \hat{x}\delta(\rho)$ for the H-polarization case. (We abbreviate the cases as E-pol and H-pol, respectively.) Thus the spectral domain Green's function for auxiliary vector potential $\vec{A}$ in 2D layers can be written as [5]

$$\tilde{G}_{yy}^A = \frac{\mu_i}{2jk_{z_i}} \left\{ \begin{array}{l} e^{-jk_{z_i}|z-z'|} + \tilde{R}_{TE}^{i,i+1}e^{-2jk_{z_i}(d_i-h)}M_i^{TE}e^{jk_{z_i}z}e^{jk_{z_i}z'} + \tilde{R}_{TE}^{i,i+1}\tilde{R}_{TE}^{i,i-1}e^{2jk_{z_i}d_i}M_i^{TE}e^{jk_{z_i}z}e^{-jk_{z_i}z'} \\ \\ +\tilde{R}_{TE}^{i,i-1}e^{2jk_{z_i}h}M_i^{TE}e^{-jk_{z_i}z}e^{jk_{z_i}z'} + R_{TE}^{i,i-1}\tilde{R}_{TE}^{i,i+1}e^{-2jk_{z_i}d_i}M_i^{TE}e^{-jk_{z_i}z}e^{-jk_{z_i}z'} \end{array} \right\} \tag{1}$$

and the Green's function for scalar potential is

$$\tilde{G}_x^q = \frac{1}{2j\varepsilon_i k_{z_i}} \left\{ \begin{array}{l} e^{-jk_{z_i}|z-z'|} + \frac{k_i^2}{k_x^2}e^{-2jk_{z_i}(d_i-z')}\gamma_1 e^{jk_{z_i}(z-z')} + \frac{k_i^2}{k_x^2}e^{-2jk_{z_i}d_i}\gamma_2 e^{jk_{z_i}(z-z')} \\ \\ -\tilde{R}_{TM}^{i,i+1}M_i^{TM}e^{-2jk_{z_i}(d_i-z')}e^{jk_{z_i}(z-z')} + \tilde{R}_{TM}^{i,i+1}M_i^{TM}\tilde{R}_{TM}^{i,i-1}e^{-2jk_{z_i}d_i}e^{jk_{z_i}(z-z')} \\ \\ +\frac{k_i^2}{k_x^2}e^{-2jk_{z_i}z'}\beta_1 e^{-jk_{z_i}(z-z')} + \frac{k_i^2}{k_x^2}e^{-2jk_{z_i}d_i}\gamma_2 e^{-jk_{z_i}(z-z')} \\ \\ -e^{-2jk_{z_i}z'}\tilde{R}_{TM}^{i,i-1}M_i^{TM}e^{-jk_{z_i}(z-z')} + \tilde{R}_{TM}^{i,i-1}M_i^{TM}\tilde{R}_{TM}^{i,i+1}e^{-2jk_{z_i}d_i}e^{-jk_{z_i}(z-z')} \end{array} \right\} \tag{2}$$

where $\gamma_1 = \tilde{R}_{TE}^{i,i+1}M_i^{TE} + \tilde{R}_{TM}^{i,i+1}M_i^{TM}$, $\gamma_2 = \tilde{R}_{TE}^{i,i+1}M_i^{TE}\tilde{R}_{TE}^{i,i-1} - \tilde{R}_{TM}^{i,i+1}M_i^{TM}\tilde{R}_{TM}^{i,i-1}$, $\beta_1 = \tilde{R}_{TE}^{i,i-1}M_i^{TE} + \tilde{R}_{TM}^{i,i-1}M_i^{TM}$ which they are applicable for both E and H polarization cases, respectively which they are applicable for both E and H polarization cases, respectively. Additionally $k_{zi} = \sqrt{k_i^2 - k_x^2}$ and k_x are the spectral domain parameters (k_x plane) and $\tilde{R}_{TE(TM)}^{i,i-1}$ and $\tilde{R}_{TE(TM)}^{i,i+1}$ are the reflection coefficients from the lower and upper regions when the source in the i-th region and $\tilde{M}_i^{TE(TM)}$ is related to the reflection coefficients [5].

The closed form spatial domain counterpart can be formed by the inverse Fourier transform which is given by the relation

$$G_{yy}^A(G_x^q) = \frac{1}{2\pi} \int_{-\infty}^{\infty} dk_x e^{-jk_x x} \tilde{G}_{yy}^A(\tilde{G}_x^q), \tag{3}$$

where G_{yy}^A and G_x^q are spatial, $\tilde{G}_{yy}^A$ and $\tilde{G}_x^q$ are the spectral domain Green's functions, respectively. Sommerfeld integration path (SIP) is used in equation (3), [5] yet this integral have no analytical solution so time consuming numerical computation is required. Nevertheless, if the spectral Green's function is rewritten with complex exponentials of k_{zi}, then we formulate the Fourier transformed integrals in (3) in terms of Hankel's functions that using the identity

$$H_0^{(2)}(k_i\rho) = \frac{1}{\pi} \int_{-\infty}^{\infty} \frac{e^{-jk_x x}e^{-jk_{zi}|z|}}{k_{zi}} dk_x, \tag{4}$$

where $k_{zi} = \sqrt{k_i^2 - k_x^2}$ and $\rho = \sqrt{x^2 + z^2}$ and $H_0^2(k_i\rho)$ is zero order and second kind Hankel function. Thus the closed-form spatial Green's functions are obtained by employing the exponential approximation of the spectral Green's functions within the framework of the Generalized Pencil of Function (GPOF) [5]. 2D Hankel function transformation of the spectral domain Green's function is applied [5] after cumbersome one-level approach, i.e., sampling the function to be approximated along the modified integration path. Hence the carefully selected exponential functions should introduce little error when the GPOF substitutes in the original function. Using the equation (4) in the exponential expansion of the spectral Green's function above, we obtain the closed form spatial domain Green's function as

$$G_{yy}^A(x, z, z') = -\frac{j\mu_i}{4} \left\{ \begin{array}{l} H_0^{(2)}\left(k_i\sqrt{x^2 + (z-z')^2}\right) \\[2mm] + \sum_{tyy=1}^{M} b_{tyy}^{(1)} H_0^{(2)}\left(k_i\sqrt{x^2 + (z+z'+j\alpha_{tyy}^{(1)})^2}\right) \\[2mm] + \sum_{tyy=1}^{M} b_{tyy}^{(2)} H_0^{(2)}\left(k_i\sqrt{x^2 + (z-z'+j\alpha_{tyy}^{(2)})^2}\right) \\[2mm] + \sum_{tyy=1}^{M} b_{tyy}^{(3)} H_0^{(2)}\left(k_i\sqrt{x^2 + (z+z'-j\alpha_{tyy}^{(3)})^2}\right) \\[2mm] + \sum_{tyy=1}^{M} b_{tyy}^{(4)} H_0^{(2)}\left(k_i\sqrt{x^2 + (z-z'-j\alpha_{tyy}^{(4)})^2}\right) \end{array} \right\}, \tag{5}$$

where x and z are the coordinates and also b_{tyy}^k and α_{tyy}^k are coefficients of the GPOF in exponential formulation technique, and where $k = 1,2,3,4$ and $t_{yy} = 1,2,..,M$. M is a predefined parameter prior to the GPOF algorithm. The α_{tyy}^k is a complex number $\alpha_{tyy}^k = p_t^k + iq_t^k$ where p_t^k and q_t^k are both real. The

same procedure can be applied for G_x^q and spatial domain Green function for H-polarization can be written as

$$G_x^q(x, z, z') =$$

$$\frac{1}{j4\varepsilon_i} \left\{ \begin{array}{l} H_0^{(2)}\left(k_i\sqrt{x^2 + z^2}\right) \\[2mm] + \sum_{txq=1}^{M} b_{txq}^{(1)} H_0^{(2)}\left(k_i\sqrt{x^2 + (z + z' + j\alpha_{txq}^{(1)})^2}\right) + \sum_{txq=1}^{M} b_{txq}^{(2)} H_0^{(2)}\left(k_i\sqrt{x^2 + (z - z' + j\alpha_{txq}^{(2)})^2}\right) \\[2mm] - \sum_{txq=1}^{M} b_{txq}^{(3)} H_0^{(2)}\left(k_i\sqrt{x^2 + (z + z' + j\alpha_{txq}^{(3)})^2}\right) + \sum_{txq=1}^{M} b_{txq}^{(4)} H_0^{(2)}\left(k_i\sqrt{x^2 + (z - z' + j\alpha_{txq}^{(4)})^2}\right) \\[2mm] + \sum_{txq=1}^{M} b_{txq}^{(5)} H_0^{(2)}\left(k_i\sqrt{x^2 + (z + z' - j\alpha_{txq}^{(5)})^2}\right) + \sum_{txq=1}^{M} b_{txq}^{(6)} H_0^{(2)}\left(k_i\sqrt{x^2 + (z - z' - j\alpha_{txq}^{(6)})^2}\right) \\[2mm] - \sum_{txq=1}^{M} b_{txq}^{(7)} H_0^{(2)}\left(k_i\sqrt{x^2 + (z + z' - j\alpha_{txq}^{(7)})^2}\right) + \sum_{txq=1}^{M} b_{txq}^{(8)} H_0^{(2)}\left(k_i\sqrt{x^2 + (z - z' - j\alpha_{txq}^{(8)})^2}\right) \end{array} \right\}, \tag{6}$$

where b_{txq}^k and α_{txq}^k are the coefficients of the GPOF in exponential formulation technique, and where $k = 1,2,3,4,5,6,7,8$, $t_{xq} = 1,2,\ldots,M$, and M is a parameter predefined prior to the GPOF algorithm. α_{txq}^k is a complex number such that $\alpha_{txq}^k = p_t^k + iq_t^k$ where p_t^k and q_t^k are both real.

3. The methods of moments with sinc basis and testing

Here we used both GPOF technique and sinc functions to solve our integral equation when the MoM technique is applied. The GPOF is used to approximate the spectral domain Green's functions to the exponential expansions and then these exponential expansions can be used to obtain the closed form spatial domain Green's function by using the equation (3). This sinc based MoM is applied to the strip scattering in the layered medium for both E and H polarization cases given below.

a) E polarization case: Let the PEC strip in the i-th layer shown in the Figure 1 be illuminated by a plane electromagnetic wave. Our goal is to solve basically the IE in terms of field and current, that is to solve

$$E_y^s = -j\omega(G_{yy}^A * J_y) = -j\omega \int_0^{2w} J_y(x') G_{yy}^A(x - x', z, z') dx' \quad x \in M, \tag{7}$$

where $E_y^s = -E_y^{in}$ and E_y^{in} is incident electric field and symbol (*) refers to usual convolution. Notice that equation (7) is imposed on strip surfaces. We employ the MoM procedure with sinc functions to solve the above equation. For this, the unknown surface current density is expanded by orthogonal sinc functions (see Appendix for further details) as

$$J_y(x) \cong \sum_{n=0}^{N} a_n \sin c(2Wx - n), \tag{8}$$

where the sinc functions are defined in the spatial domain and W is the bandwidth of the sinc functions in a counterpart frequency domain; N is the total number points representing sinc's peak positions for a site n

and a_n is coefficients to be determined. We have also $Nt_x = 2w$, with $t_x = 1/(2W)$. Then using the current expansion the original IE in (7), we get the function

$$E_y^{in}(x, z) = j\omega \sum_{n=0}^{N} a_n \int_{-\infty}^{\infty} \sin c(2Wx' - n)G_{yy}^A(x - x', z, z')dx'. \tag{9}$$

After testing both sides by sinc functions (using the Galerkin method) and changing variables $x - x\prime = u$, we get the relation

$$\int\limits_{-\infty}^{\infty} E_y^{in}(x, z) \sin c(2Wx - m)\, dx$$
$$= j\omega \sum_{n=0}^{N} a_n \int\limits_{-\infty}^{\infty} G_{yy}^A(u, z, z') \left(\int\limits_{-\infty}^{\infty} \sin c(2Wx - m) \sin c(2W(x - u) - n)dx \right) du, \tag{10}$$

where the integral inside the right hand side bracket is a convolution. We can reformulate this by using the orthogonally and convolution (of two sinc functions is also another sinc; see Appendix) that $E_y^{in}(x)$ reduces to

$$E_y^{in}(t_x m, z) = j\omega \sum_{n=0}^{N} a_n \int_{-\infty}^{\infty} \sin c(2Wx - n + m)G_{yy}^A(x, z, z')dx, \tag{11}$$

which can be written in a matrix form

$$[A_{mn}][a_n] = [B_m], \tag{12}$$

where

$$A_{mn} = j\omega \begin{cases} t_x G_{yy}^A(|n - m|t_x, z, z') + \text{error} & |n - m| \geq L \\ \\ \int_{-\infty}^{\infty} \sin c(2Wx - n + m)G_{yy}^A(x, z, z') & |n - m| < L \end{cases} \tag{13}$$
$$B_m = E_y^{in}(t_x m, z),$$

and where L is a small integer number. The convergence of the above defined integral will be discussed shortly. The GPOF technique produces error close to machine precision, i.e. very low error rate [5], but the sinc function integrals produce relative error of about 0.5% to 1% (see section 4). These magnitude errors are in a better range compared to the usual MoM; yet the written code consumes very little CPU time, even with an ordinary PC.

   b) H polarization case: Similar layered geometry shown in the Figure 1 is considered. The basic IE for this case is

$$E_x^{inc} = j\omega \left[\vec{J}(\vec{r}) * G_{yy}^A(\vec{r}) \right] + \frac{\partial}{\partial x} \left[\frac{\nabla \cdot \vec{J}}{j\omega} * G_x^q(\vec{r}) \right], \tag{14}$$

where the above integral equation given in (14) has a different boundary condition. After applying the

convolution integral operators to the equation (14), it takes the form

$$
\begin{aligned}
E_x^{in}(x,z) = \quad & j\omega \int\limits_0^{2w} J_x(x') G_{yy}^A(x-x',z,z')dx' \\
& + \frac{1}{j\omega}\left(\frac{\partial J_x(x')}{\partial x'} G_x^q(x-x',z,z')\Big|_0^{2w} \right) \\
& - \frac{1}{j\omega}\int\limits_0^{2w} \frac{\partial^2 J_x(x')}{\partial x'^2} G_x^q(x-x',z,z')dx',
\end{aligned}
\tag{15}
$$

where $J_x(x)$ denotes the surface current distribution. Also G_{yy}^A and G_x^q are the required Green's functions of the layered geometry (see section 2).

In the equation (15), the derivatives can be evaluated by using the finite difference manner and also by the cost of the error, it comes from derivative expression. The unknown surface current distribution is again approximated by orthogonal sinc functions as performed in the E-pol case:

$$
J_x(x) \cong \sum_{n=1}^{N-1} a_n \sin c(2Wx - n),
\tag{16}
$$

where the sinc functions are defined in the spatial domain and W is the bandwidth of these sinc functions in the frequency domain. The N-1 is the number of total sample points on the strip and due to the boundary conditions on the surface current density, at the initial and final points on the strip, the current density is zero. We have also $Nt_x = 2w$. Then using the current expansion (16) in the original IE given in (15), we get

$$
\begin{aligned}
E_x^{in}(x,z) = \quad & j\omega \sum_{n=1}^{N-1} a_n \int\limits_{-\infty}^{\infty} \sin c(2Wx' - n) G_{yy}^A(x-x',z,z')dx' \\
& + \frac{1}{j\omega}\left(\frac{\partial J_x(x')}{\partial x'} G_x^q(x-x',z,z')\Big|_0^{2w} \right) \\
& - \frac{1}{j\omega}\sum_{n=1}^{N-1} \frac{a_{n+1}-2a_n+a_{n-1}}{(t_x)^2} \int\limits_{-\infty}^{\infty} \sin c(2Wx' - n) G_x^q(x-x',z,z')dx',
\end{aligned}
\tag{17}
$$

where we have the residual error to be minimized.

So we tested both sides of equation (17) by the sinc functions and then applying change of variables, one can find a convolution of the sinc functions similar to that of equation (10) for the E-polarization case. Then finally all the terms are arranged into an algebraic matrix equation, as is done in MoM. The function we get is

$$
t_x E_x(pt_x,z) = j\omega t_x [A_{np}][a_n] + \frac{2}{j\omega t_x}[A_{np}^q][a_n] + \frac{j}{\omega t_x}[\gamma_{np}][a_n].
\tag{18}
$$

In above equation (18), A_{np} matrix can be written as

$$
A_{np} = \begin{cases} t_x G_{yy}^A(|p-n|t_x,z,z') + \text{ error}, & |p-n| \geq L, \\[2ex] \int_{-\infty}^{\infty} \sin c(2Wu - p + n) G_{yy}^A(|u|,z,z')du, & |p-n| < L, \end{cases}
\tag{19}
$$

where L is a small integer. Also A_{np}^q matrix including G_x^q can be evaluated as

$$A_{np}^q = \begin{cases} t_x G_x^q(|p-n|t_x, z, z') + \text{error}, & |p-n| \geq L, \\[2ex] \int_{-\infty}^{\infty} \sin c(2Wu - p + n) G_x^q(|u|, z, z') du, & |p-n| < L. \end{cases} \qquad (20)$$

In equation (18), the third term in the right hand side can be written as the sum of matrices,

$$\gamma_{np} = F_{np} + G'_{np} \qquad (21)$$

where

$$F_{np} = [C_p | A_{(n-1)p}^q], \qquad (22)$$

$$G_{np} = [A_{(n+1)p}^q | D_p]. \qquad (23)$$

Also, matrix coefficients C_p and D_p are given as

$$C_p = \int_{-\infty}^{\infty} \sin c(2Wu - p) G_x^q(|u + 2w|, z, z') du, \qquad (24)$$

$$D_p = \int_{-\infty}^{\infty} \sin c(2Wu - p) G_x^q(|u|, z, z') du. \qquad (25)$$

The above described mainly depends on the dense mesh of the sinc functions; but when the sinc functions become narrow due to the quasi-localized property [23] of the special function, peak values of the sinc become more effective in the integral.

Also here in the H-polarization case the derivatives are expressed as finite difference manner. Our code runs in reasonable time with an ordinary PC. Notice that this way of MoM solution can easily be extended for multi-strip case in layered medium. The convergence of this integral, i.e. similar to the free space case, is discussed in section 4.

4.   Sinc integral approximations

Constructing the matrix integrals of the MoM for layered medium, the integrand for the free space term, i.e., the first term of the spectral Green's function, can be approximated by Hankel function again and the error level goes to zero as W increases and even stronger for nonzero $|z$-$z'|$ [20, 21, 22, 24]. All four terms representing the scattering part in the spatial domain under the integral can be written and then it can be expressed in a compact form approximately as

$$\int_{-\infty}^{\infty} \sin c(2Wx - n + m) H_0^{(2)}(k_i \sqrt{x^2 + (A - i\alpha_t^k)^2}) \, dx = t_x H_0^{(2)}(k_i \sqrt{(n-m)^2 t_x^2 + (A - i\alpha_t^k)^2}) + \text{Error}, \quad (26)$$

where A and α_t^k (symbolized as α_{tyy}^k or α_{txq}^k) are arranged such that the equation (26) models the four different the scattered parts of G_{yy}^A (or G_x^q). We have here $A \geq 0$ and real but α_t^k's are complex numbers. Notice that A is function of both z and z' and n and m are site numbers.

The aim is to approximate this integral with simple Hankel function such as in the right side of the equation (26) that can be useful for a negligible error. To find error criteria, we applied Parseval's relation to the both sides. After that we found similar integrands and then we can subtract these two from each other and thus the absolute error is given as follows by the modified integral limits,

$$Error = -t_x \int_W^\infty \underbrace{\frac{4}{\sqrt{k_i^2 - 4\pi^2 f_x^2}}}_{k_{zi}} \underbrace{e^{-jk_{zi}(A-j\alpha_t^k)}}_{\gamma} \cos \frac{\pi f_x}{W} |n-m| \, df_x, \tag{27}$$

where $k_{zi} = \sqrt{k_i^2 - k_x^2}$ and $k_x = 2\pi f_x$. Define the exponential term as $\gamma = \mathrm{e}^{-jk_{zi}(A-j\alpha_t^k)}$. Substituting the previously defined parameter α_t^k in γ, then inserting it in the equation (27), and expanding square root, since $k_i^2 << 4\pi^2 f_x^2$ (doing so increases error), we get

$$Error \cong -t_x i(2/\pi) \int_W^\infty e^{-2\pi f_x (A+q_t^k)} \, e^{j2\pi f_x p_t^k} \, \frac{\cos(\pi f_x |n-m|/W)}{f_x} \, df_x. \tag{28}$$

In fact, already on this level, very low error limit is reached with increasing W. Note also that, when $A + q_t^k > 0$, the integral above converges due to an exponential decaying factor. For $A + q_t^k < 0$, the other branch has to be chosen for convergence. In addition to the exponentially convergent factor, the error in question has also an exponentially oscillating factor $e^{j2\pi f_x p_t^k}$ as well. This rapidly oscillating factor contributes greatly to the convergence, even in absence of exponential decay. If $\alpha_t^k = p_t^k + iq_t^k = 0$, $A = 0$ and $z = z' = 0$ for all values of t and k (free space case), we would obtain the same relative error formula in [22]. So we conclude that our error is smaller then 1% for $L = 1$ or 0.5% for $L = 2$, where $L = |n\text{-}m|$. Note that our analyses work for $L > = 1$; *otherwise,* for $L = 0$ or $n = m$, it is recommended that the original error integral of Hankel function equation (13) has to be taken numerically. For $L \geq 1$, the upper bound of the absolute error reduces to

$$Error \leq \frac{i}{\pi W} \, Ci(\pi|m-n|). \tag{29}$$

where the relative error can be found by using the above absolute error by diving it to just the right hand side of the Hankel function expression.

5. Numerical results

The above formulation is performed utilizing the Sinc-Galerkin MoM whose error along the computation significantly reduces as W increases. To check this, we have done number of computations for single/multi strip geometries in the layered medium. We expect also to achieve significantly fast performance in our computation. To confirm its performance, we deliberately used relatively modest computational facility and implement the regular MoM procedure (which is quite slower than its later versions). Simulations were carried out on an AMD Athlon 3200+ 2.0 GHz processor with 1.00 GB RAM under Matlab®7.0 program package operated under the Windows operating system.

As we have developed general formulation in the previous chapters, we apply it now to some specific geometries to verify our formulation. Producing matrix elements through transforming sinc integrals to Hankel functions, we reduced successfully computation time as we have targeted.

In Figure 1, the general layered media is shown by the different ε_i values defined in each region, separately. Thickness of each layer may vary depending on the problem's geometry. In Figure 2, the three strips with different locations are considered inside the slab, i.e. three region case where the strips are embedded in the slab. In the same figure, in part (b), two layer geometry is given and the single strip located at the upper region. The angle ϕ appearing in the radiation patterns in the numerical results part is the scattering angle and is shown in Figure 2(b). Also, angle θ^{inc} shows the incident direction of the incoming electromagnetic plane wave which excites this scattering problem. Width of the strip '$2w$' may vary, depending on the problem. The Figure 1 and Figure 2 define the geometry of the problems we have studied here.
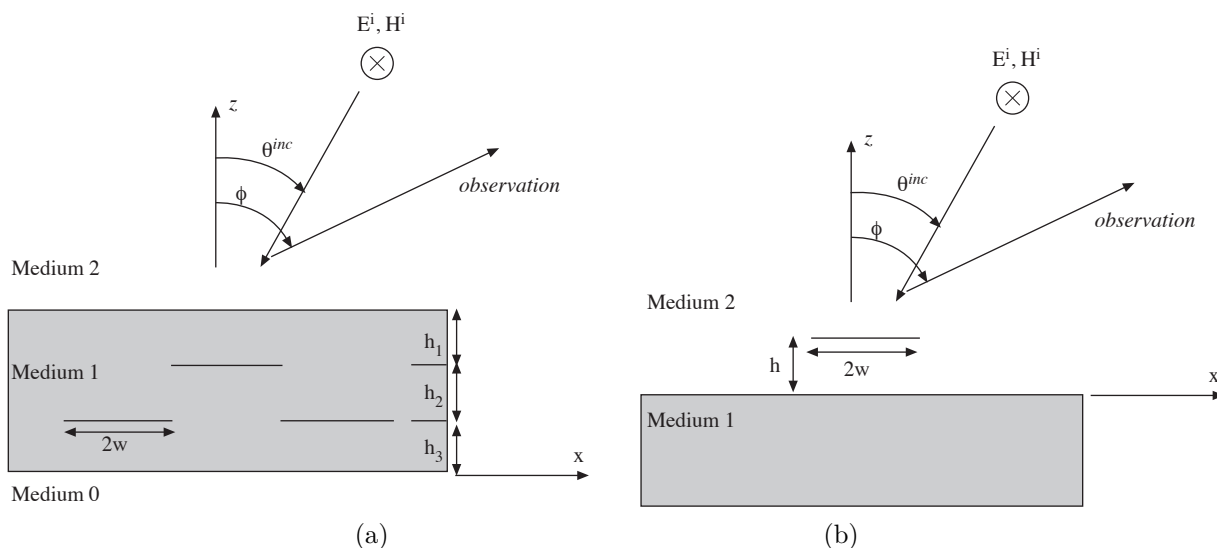

Figure 2. Geometric configuration: (a) three strip and three layer geometry; (b) one strip and two layer geometry.

In Figure 3, E-polarized plane wave is incident normally to the geometry of Figure 2(a) and the results are given on the same plot with the sinc based MoM solution and the pulse type basis functions used in the ordinary Galerkin procedure. Both the current density magnitudes of our method and MoM using pulse type functions are consistent with each other shown in the same figure (Figure 3). H-polarized case for the same geometry is presented in Figure 4 where the sinc based-MoM and regular triangular basis MoM are presented in the same plot. In these figures, we observed that the error is higher in the E-pol case than H-pol, since E polarization has singular behavior near edges that some current (especially sinc functions located near the edges) persists out of the strip in E polarization (see Figure 3).

Keeping the same geometry (Figure 2(b)), single horizontal strip located at the interface between 2 half-spaces, the current densities for E and H polarization excitations are calculated. Parameters chosen are: $\varepsilon_{r1} = 4$ and $\varepsilon_{r2} = 1$ for relative dielectric constants; width of the strip is $2w = 4\lambda$, the height of the strip from the interface is set to 0, thus the current densities for E and H polarization excitations are obtained using sinc based MoM. Real and imaginary parts of current densities are given in Figure 5 and 6, respectively. Comparing results with those found in [5], excellent aggreement is observed.

Once the current densities are obtained, one can obtain the far field patterns of radiation arising from the strip. Both E-polarized and H-polarized incident wave cases are considered in the following figures. First the current density of the strip is computed, then using far field approximations, scattered fields are plotted in

Figures 7 and 8. For relative dielectric constants, $\varepsilon_{r1} = 4$, $\varepsilon_{r2} = 1$ and the width of the strips is $2w = 0.5\lambda$, with normal incidence.
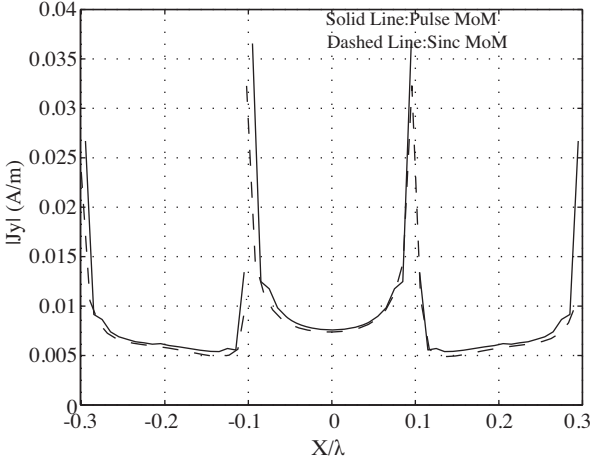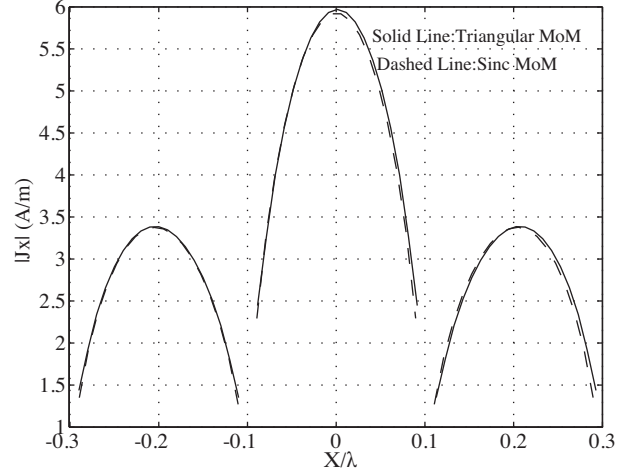

Figure 3. Magnitudes of the current densities for E-polarization on the three strips for the three regions, i.e., the strips inside the slab with $\varepsilon_{r0} = \varepsilon_{r2} = 1$ and $\varepsilon_{r1} = 4$ also $2w = 0.2\lambda_2, h_1 = h_2 = h_3 = 0.1\lambda_2$ and $\theta^{inc} = 0$.

Figure 4. Magnitudes of the current densities for H-polarization on the three strips for the three regions, i.e., the strips inside the slab with $\varepsilon_{r0} = \varepsilon_{r2} = 1$ and $\varepsilon_{r1} = 4$ also $2w = 0.2\lambda_2$, $h_1 = h_2 = h_3 = 0.1\lambda_2$ and $\theta^{inc} = 0$.
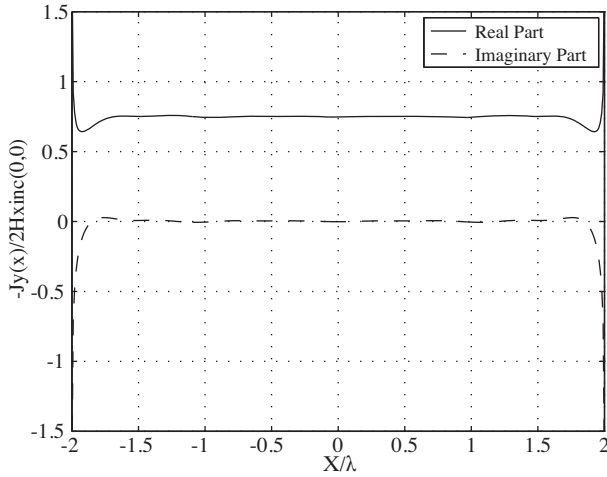
Figure 5. Real and imaginary parts of the normalized current densities for E-polarization excitation. $\varepsilon_{r2} = 1$, $\varepsilon_{r1} = 4$, $2w = 4\lambda_2$, $h = 0$, $\theta^{inc} = 0$.
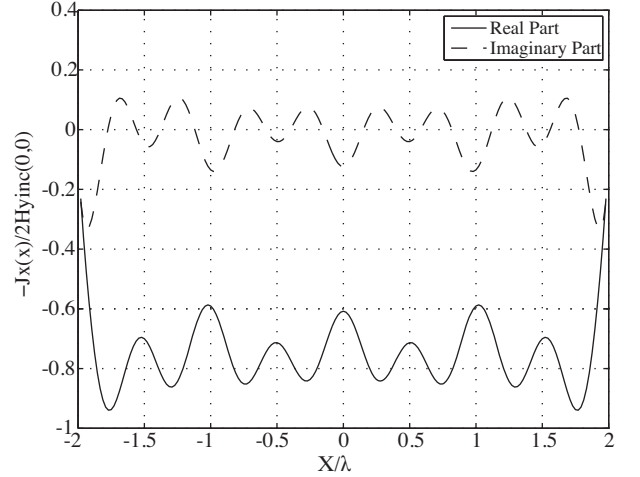
Figure 6. Real and imaginary parts of the normalized current densities for H-polarization excitation. $\varepsilon_{r2} = 1$, $\varepsilon_{r1} = 4$, $2w = 4\lambda_2$, $h = 0$, $\theta^{inc} = 0$.

Furthermore (in Figure 7), the heigth of the strip from the interface is taken as $h = 5\lambda$, 10λ or 15λ, given as parts (a), (b) and (c), respectively. For similar geometry, the same dielectric constants and the incidence angles are used, except for the height of the strip is taken as 5λ and the width of the strip, $2w$, is chosen as 0.5λ, 2λ and 5λ as parts (a), (b) and (c) of Figure 8, respectively. We clearly see that in the Figure 7 and 8, the number of oscillations is increased and level of radiation pattern became higher while increasing the strip height from the interface and the width of the strip, respectively.
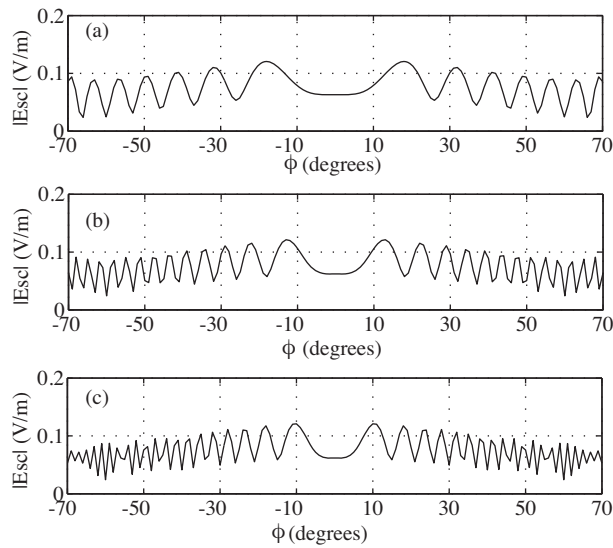
Figure 7. Far field patterns of one strip on the two layer geometry problem for E-polarization excitation with parameters $\varepsilon_{r2} = 1$, $\varepsilon_{r1} = 4$, $2w = 0.5\lambda_2$, $h = 5\lambda_2$, $\theta^{inc} = 0$ for (a), $\varepsilon_{r2} = 1$, $\varepsilon_{r1} = 4$, $2w = 0.5\lambda_2$, $h = 10\lambda_2$, $\theta^{inc} = 0$ for (b) and $\varepsilon_{r2} = 1$, $\varepsilon_{r1} = 4$, $2w = 0.5\lambda_2$, $h = 15\lambda_2$, $\theta^{inc} = 0$ for (c).
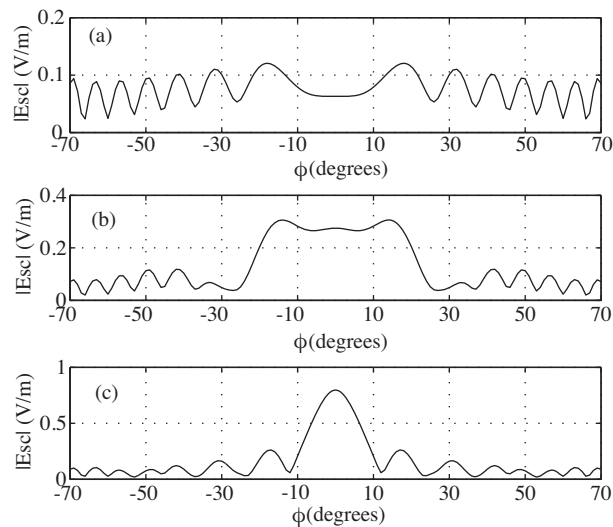

Figure 8. Far field patterns of one strip on the two layer geometry problem for E-polarization excitation with parameters $\varepsilon_{r2} = 1$, $\varepsilon_{r1} = 4$, $2w = 0.5\lambda_2$, $h = 5\lambda_2$, $\theta^{inc} = 0$ for (a), $\varepsilon_{r2} = 1$, $\varepsilon_{r1} = 4$, $2w = 2\lambda_2$, $h = 5\lambda_2$, $\theta^{inc} = 0$ for (b) and $\varepsilon_{r2} = 1$, $\varepsilon_{r1} = 4$, $2w = 5\lambda_2$, $h = 5\lambda_2$, $\theta^{inc} = 0$ for (c).

In Figure 9 and 10, the far field patterns of the scattered H-field are given. The parameters of the Figure 9 and Figure 10 are the same as used in the previous Figures 7 and 8. As in the E-pol case, similar in level of radiation pattern and number of oscillations are also observed. Comparing scattered fields of E and H polarizations, we obtained some oscillations. But levels of radiation pattern are greater in H-pol case than in E-pol case. Since the current densities obtained in H-pol case are extremely larger than E-pol case.
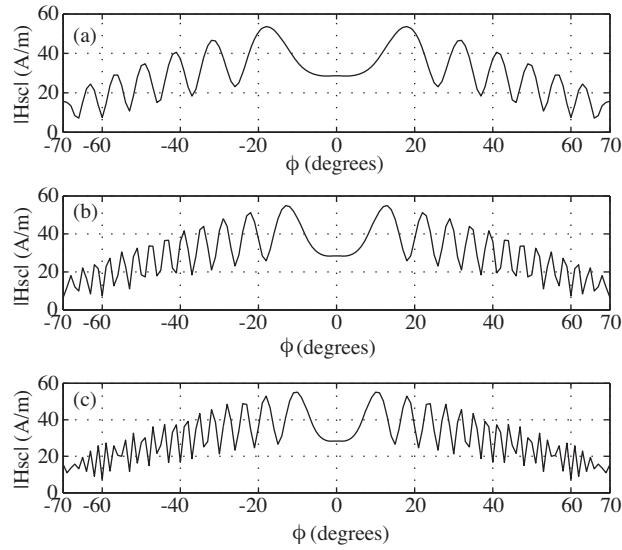
Figure 9. Far field patterns of one strip on the two layer geometry problem for H-polarization excitation with parameters $\varepsilon_{r2} = 1$,$\varepsilon_{r1} = 4$, 2w = $0.5\lambda_2$,h = $5\lambda_2$, $\theta^{inc} = 0$ for (a), $\varepsilon_{r2} = 1$,$\varepsilon_{r1} = 4$, 2w = $0.5\lambda_2$, h = $10\lambda_2$, $\theta^{inc} = 0$ for (b) and $\varepsilon_{r2} = 1$, $\varepsilon_{r1} = 4$, 2w = $0.5\lambda_2$, h = $15\lambda_2$, $\theta^{inc} = 0$ for (c).
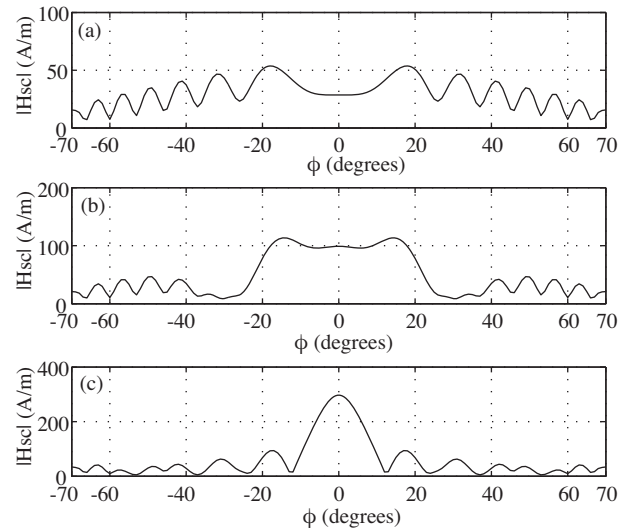

Figure 10. Far field patterns of one strip on the two layer geometry problem for H-polarization excitation with parameters $\varepsilon_{r2} = 1$,$\varepsilon_{r1} = 4$, 2w = $0.5\lambda_2$,h = $5\lambda_2$, $\theta^{inc} = 0$ for (a), $\varepsilon_{r2} = 1$, $\varepsilon_{r1} = 4$, 2w = $2\lambda_2$, h = $5\lambda_2$, $\theta^{inc} = 0$ for (b) and $\varepsilon_{r2} = 1$, $\varepsilon_{r1} = 4$, 2w = $5\lambda_2$, h = $5\lambda_2$, $\theta^{inc} = 0$ for (c).

In Table 1 and Table 2 the computation times for the geometry shown in Figure 2(b) are presented. The resulting CPU times are indeed shorter than what we expected. Our code worked quite faster regarding to the regular MoM's performance for both E-polarized and H-polarized cases. We achieved better performance even with a MATLAB 7.0 code running on a modest PC when compared with the results obtained with usual facilities such as a fast sun system as in [5]. Significant reduction of an overall CPU time data is displayed in

Table 2. The results obtained from our spatial domain formulation are proven to be better in many performance regards than those of the results found in the literature (we already performed to compare with our results).

Table 1

Number of sample points on each 0.2λ width strip.	CPU Time of overall program in seconds, for a 3-strip case, each strip with 0.2λ width (Geometry in Figure 2(a)). Sinc type basis and test functions in MoM for E-pol case.	CPU Time of overall program in seconds, for a 3-strip case, each strip with 0.2λ width (Geometry in Figure 2(a)). Pulse type basis and test functions in MoM for E-pol case.
N=10	063 s	072 s
N=20	124 s	239 s
N=40	254 s	300 s

Table 2

Number of sample points on each 0.2λ width strip.	CPU Time of overall program in seconds, for a 3-strip case, each strip with 0.2λ width (Geometry in Figure 2(a)). Sinc type basis and test functions in MoM for H-pol case.	CPU Time of overall program in seconds, for a 3-strip case, each strip with 0.2λ width (Geometry in Figure 2(a)). Triangular type basis and test functions im MoM for H-pol case.
N=10	114 s	525 s
N=20	261 s	2069 s
N=40	642 s	8010 s

6. Conclusion

The sinc function based methods of moments are applied to a planar layered media containing a single or multi strips in various geometries for both polarization cases. The sinc type basis functions are used as in the Galerkin sense. Far field patterns of fields are examined and effects of strip width and distance to the interfaces are monitored. We conveniently exploited the properties of the sinc functions in our formulation. We showed that the error is reduced under a specified limit where the sinc basis bandwidth increases. When compared to layered scattering regular MoM studies obtained before, the presented formulation provides an accurate solution faster with better accuracy. Hence E and H polarization results compared with available literature, we get striking consistency. We are currently developing our code to simulate 3D scattering problems for several planar geometries.

Appendix

The set of the sinc functions defined in section 3 constitutes a complete orthogonal set and this orthogonally can be represented as

$$\int_{-\infty}^{\infty} \sin c(2Wx - n) \sin c(2Wx - m)dx = \begin{cases} 1/(2W) & \text{if} \quad n = m \\ 0 & \text{if} \quad n \neq m, \end{cases} \tag{A1}$$

where n and m are integer numbers and W is the frequency domain bandwidth of given sinc functions written in the spatial domain. The convolution of two sinc functions located at different points in the spatial domain produces again a sinc function mounted at the location of their difference:

$$\int_{-\infty}^{\infty} \underbrace{\sin c(2Wx' - n)}_{g_1(x')} \underbrace{\sin c(2W(x - x') - m)}_{g_2(x' - x)} \, dx' = (1/(2W)) \underbrace{\sin c(2Wx - n + m)}_{g_3(x)}, \tag{A2}$$

where n and m are integer numbers and W is the bandwidth of these sinc functions. Equation (A2) can also be written as

$$g_1(x) * g_2(-x) = (1/(2W)) \, g_3(x). \tag{A3}$$

Proof of this relation follows from taking the Fourier transform of both sides.

References

[1] R. F. Harrington, Time Harmonic Electromagnetic Fields, New York, McGraw Hill, 1961

[2] Jian-She Wang, Nathan Ida, "3 D finite element calculation of harmonic electromagnetic fields," IEEE transactions on magnetics, vol. 26, No:2 March 1990

[3] Shaobin Liu; Naichang Yuan; Jinjun Mo, "A novel FDTD formulation for dispersive media," Microwave and Wireless Components Letters, IEEE, Volume 13, Issue 5, May 2003 Page(s): 187 – 189

[4] Feng Ling; Jiming Song; Jian-Ming Jin, "Multilevel fast multipole algorithm for analysis of large-scale microstrip structures," Microwave and Guided Wave Letters, IEEE [see also IEEE Microwave and Wireless Components Letters], Volume 9, Issue 12, Dec 1999, pp. 508–510.

[5] M. I. Aksun, F.Çalışkan and L. Gurel, "An efficient method for electromagnetic characterization of 2-D geometries in stratified media" IEEE Trans. On AP, vol. 50, no. 5, May 2002.

[6] Noyan Kinayman and M. I. Aksun, "Efficient evaluation of the MoM matrix entries for planar geometries in multilayer media," IEEE Trans. Microwave Theory Tech., vol. MTT-48, pp. 309–312, Feb. 2000.

[7] M. I. Aksun, "A robust approach for the derivation of closed-form Green's functions," IEEE Trans. Microwave Theory Tech., vol. MTT-44, pp. 651–658, May 1996.

[8] A.Saadatmandi, M.Razzaggi and M. Dehghan, "Sinc-Collocation methods for the solution of Hallen's integral equation" Journal of Electromagnetic Waves and Applications, vol. 19, no. 2, pp. 245–256, 2005.

[9] F. Stenger, "Numerical methods based on the sinc and analytic functions," Springer-Verlag, New York 1993.

[10] Lund, J. and K. Bowers, "Sinc methods for quadrature and differential equations," SIAM, Philadelphia 1992.

[11] E.X. Huang and A.K. Fung, "An application of sampling theorem to moment method simulation in surface scattering," Journal of Electromagnetic Waves and Applications, vol. 20, no. 4, pp. 531–546, 2006.

[12] Kalhor, H.A and M.R. Zunoubi, "Electromagnetic scattering and absorption by arrays of lossless/lossy metallic or dielectric strips," Journal of Electromagnetic Waves and Applications, vol. 19, no. 4, pp. 497–512, 2005

[13] S. Wang, X. Guan, D. Wang, X. Ma and Y. Su, "Electromagnetic scattering by mixed conducting/dielectric objects using higher-order MoM," PIER, 66, 51–63, 2006.

[14] M. D. Arnold, "An efficient solution for scattering by a perfectly conducting strip grating," Journal of Electromagnetic Waves and Applications, vol. 20, no.7 891-900 2006.

[15] X. Liu, B.Z. Wang and S. Lai, "Element-free Galerkin method in electromagnetic scattering field computation" Journal of Electromagnetic Waves and Applications vol. 21 no.14 1915-1923 2007.

[16] A. Danideh, R. Sadeghi Fakr and H.R. Hassani, "Wideband co-planar microstrip patch antenna" PIER Letters vol. 4 81-89 2008.

[17] H.R. Hassani and M. Jahanbakht, " Method of moments analysis of finite phased array of aperture coupled circular microstrip patch antennas," PIERB, vol. 4, 197–210, 2008.

[18] Tretiakov, Y. and G. Pan, "Malvar wavelet based Pocklington equation solutions to thin-wire antennas and scatterers," PIER, 47, 123–133, 2004.

[19] A. Matsushima and T. Itakura, "Singular integral equation approach to plane wave diffraction by an infinite strip grating at oblique incidence," Journal of Electromagnetic Waves and Applications, vol. 4, no. 6 505–519, 1990.

[20] Fadil Kuyucuoglu, Zarife Cay, Taner Oguzer, "Scattering From the P.E.C. Flat Strip Using The Method of Moments with Sinc Basis Functions," 6th International Conference on Computational Electromagnetics (CEM 2006), 4–6 April, 2006, Aachen, Germany.

[21] Taner Oguzer, Fadil Kuyucuoglu, "Solution of Scattering Problem from a strip located in a layered media using the Method of Moments" URSI, 3th National Congress, 6–8 September, 2006, Ankara, Turkey (in Turkish).

[22] Taner Oguzer, Fadil Kuyucuoglu, "Method of Moments Solution by Using sinc-type Basis Functions for the Scattering from a Finite Number of Conducting Strip Gratings," Turkish Journal of Electrical Engineering and Computer Sciences, July 2008.

[23] G.F. Hermann, "Notes on interpolational basis functions in the method of moments," IEEE Transactions on AP, vol. 38, pp. 134–137, 1990.

[24] Kuyucuoglu F, Oguzer T, Avgin I, "Scattering from the flat strip geometries in the layered medium by using the sinc based method of moments," PIERS International conference Cambridge proceedings, 725–729, 2008.